Thermal characterization of a series of poly(vinylidenefluoride–chlorotrifluoroethylene–trifluoroethylene) terpolymer films

Hengfeng Li · Kaiyuan Tan · Zeming Hao ·
Guowen He

Abstract A number of solution-casted poly(vinylidenefluoride–chlorotrifluoroethylene–trifluoroethylene) [P(VDF–CTFE–TrFE)] terpolymer films with different CTFE content have been characterized by a series of thermal analysis techniques, including thermogravimetric analysis (TG), differential scanning calorimetry, dynamic mechanical analysis (DMA) and thermal mechanical analysis (TMA). The work intends to provide more comprehensive information about thermal behavior of these ferroelectric polymers. TG results suggest that the introduction of the CTFE units slightly decreases the thermal stability of the polymer due to the instability of C–Cl bond during heating. DMA detected a relatively weak α_a relaxation and a broad α_c relaxation in the samples of low CTFE content. These two relaxation processes completely mixed together in the sample with high CTFE content, revealing the crystalline structures in the polymer, become a more imperfect and diffuse state as CTFE units increasing. The polymer with less CTFE units possesses an enhanced stiffness due to its higher degree of crystallinity. A contraction process after a slight amount of thermal expansion upon heating is detected by TMA, due to the release of internal tensile strain/stress generated during solidification of the films. The higher crystallinity of the polymer film generated the greater strain/stress, leading to the larger degree of shrinkage. Also, the higher melting point of the polymer with less CTFE units allows the film soften at a higher temperature.

Introduction

Poly(vinylidene fluoride) (PVDF) based ferroelectric polymers are technologically important thermoplastics, which find a variety of applications in advanced electro-mechanical devices such as capacitors, transducers, actuators, sensors and non-volatile memories [1–5]. In the past few decades, PVDF based homo- and co-polymers have attracted a great deal of scientific attention due to its good mechanical properties and desirable piezoelectric, ferroelectric and pyroelectric properties [5–12]. The interesting electronic properties of PVDF originate from the presence of highly electronegative fluorine on the polymer chain and the spontaneous alignment of the C–F dipoles in the crystalline phases [13]. PVDF is a semi-crystalline polymer, its polymer chains can be packed into various crystal lattices, resulting in different crystalline phases mainly including non-polar α-phase with trans-gauche chain conformation, polar β-phase with all trans zigzag chain conformation and weakly polar γ-phase with trans-trans-trans-gauche chain conformation [6]. Among them, the β-phase has parallel dipole moments and thus is the most polar one with large spontaneous polarization and corresponding ferroelectricity and piezoelectricity, but the α-phase is the more stable and common one. This phase can be formed during simple crystallization upon cooling from the melt in quiescent conditions [14]. The switch from the non-polar to polar phases can be induced by electric field poling or mechanical stretching. During the phase transition, large differences in dipole moments and

H. Li (✉) · K. Tan · Z. Hao · G. He
School of Materials Science and Engineering,
Central South University, Changsha, Hunan 410083,
People's Republic of China
e-mail: lihengfeng@gmail.com

lattice parameters exist among different phases, leading to significant changes of dielectric constants, piezoelectric and pyroelectric coefficients, and interesting electromechanical responses. The energy barrier of the phase transition is closely related to the chain structure [15].

PVDF generally displays low electric field sensitivity in terms of its dielectric constant, piezoelectric coefficient, and electromechanical coupling efficiency at room temperature due to its high crystallinity and large crystal lattice size. Owing to its high energy barrier of the phase transition, the ferroelectric–paraelectric (F–P) phase transition (i.e., curie transition) in PVDF is absent below the melting point. By incorporating trifluoroethylene (TrFE) into PVDF, the resulting P(VDF–TrFE) copolymers are able to crystallize directly at room temperature into the ferroelectric β-phase. As the F-atom in TrFE is slightly larger than the H-atom, in the copolymer the trans bond is favored over the gauche bond due to steric hindrance occurring in the latter [10, 16]. The ferroelectricity in the P(VDF–TrFE) copolymers is evidenced by the existence of the Curie transition below the melting point [17]. However, the lowest Curie transition temperature (T_c) for P(VDF–TrFE) appears at ca. 60 °C with 45 mol% TrFE in the copolymer [16–18]. The introduction of a third bulky monomer, such as chlorotrifluoroethylene (CTFE), 1,1-chlorofluoroethylene (CFE), hexafluoropropylene (HFP), as random defects into P(VDF–TrFE), can transform the macroscopic polar domains in the copolymer to nanoclusters and further reduce or even eliminate the energy barrier of the phase transition [19–27]. Some of the resulting terpolymers show high dielectric constant, slim polarization hysteresis, and large electrostrictive response at ambient temperature and exhibit common ferroelectric relaxor behaviors with a broad dielectric peak that shifted toward higher temperatures as the frequency increased [19–27]. This is different from the copolymer, a normal ferroelectric material, in which the F–P transition does not show much frequency dependence. The unusual relaxor behaviors of the terpolymers are considered as a result of heterogeneous nanoscale polar crystalline regions where the energy barriers to reorientation are comparable to the energy of thermal motion. Conventionally, the terpolymers are produced by free-radical polymerization of the three monomers using emulsion, suspension, solution, and bulk methods; however, one major concern in these direct processes is the limited supply of TrFE monomer that is dangerous [28] in transport and storage and is very expensive. Recently, a more convenient chemical route [29–31], including VDF/CTFE copolymerization and partial reduction of chlorine in P(VDF–CTFE), is reported to synthesize the poly(vinylidene fluoride–chlorotrifluoroethylene–trifluoroethylene) [P(VDF–CTFE–TrFE)], this approach allows to tune the dielectric properties of the polymers by exquisite control over chemical compositions [29–32].

The previous researches have given the full investigation of electrical properties of the terpolymers; however, their thermal properties have not been reported in a comprehensive manner. Especially, the information on their thermal stability and thermomechanical properties is very scarce. In this study, a number of P(VDF–CTFE–TrFE) terpolymer films with different CTFE content have been characterized by a series of thermal analysis techniques, including Thermogravimetric analysis (TG), Differential scanning calorimetry (DSC), Dynamic mechanical analysis (DMA), and Thermal mechanical analysis (TMA). The work intends to provide more comprehensive information about the thermal behavior of these ferroelectric polymers.

Experimental

Materials

P(VDF–CTFE–TrFE) terpolymers with different CTFE content were synthesized by partial reduction of chlorine in P(VDF–CTFE) copolymers. The detailed synthesis processes and composition of the terpolymers have been discussed in our previous study [33]. The polymer composition is listed in Table 1.

Preparation of the terpolymer films for measurement

The predetermined amounts of polymers were fully dissolved in *N,N*-dimethylformamide (DMF) to make homogeneous solutions with the concentration of 100 mg mL^{-1}. The solutions were poured onto clean and flat glass slides; laid the slides horizontally and dried at 65 °C under vacuum for 24 h. Polymer films with thickness around 30 μm were obtained.

Characterization

TG was performed on a NETZSCH STA 449 C apparatus under argon gas flow (60.0 mL min^{-1}). The temperature ranged from 30 to 800 °C at a heating rate of 10 °C min^{-1}.

Table 1 The composition of the P(VDF–CTFE–TrFE) terpolymers

Polymer no.	Polymer composition/mol%		
	VDF	CTFE	TrFE
1	68.0	23.1	8.9
2	68.0	13.6	18.4
3	68.0	6.7	25.3
4	68.0	4.4	27.6
5	68.0	1.1	30.9

The initial sample weights were between 4.900 and 5.100 mg. DSC experiments were conducted using a NETZSCH DSC 200 F3 thermal analyzer. The sample was hermetically sealed in an aluminum pan and heated from 10 to 200 °C at a rate of 10 °C min^{-1}. The typical sample weight for DSC was 5.000 mg. The temperature of all the instruments was calibrated with indium and lead standards. For heat flow calibration, only the same indium sample was used.

DMA was carried out in a TA Instruments DMA Q800 apparatus at 1 Hz frequency with temperature varied from −50 to 120 °C at a rate of 2 °C min^{-1}, using the tensile mode. Rectangular samples were cut from the terpolymer films with 4 mm width and 25 mm distance between clamps. In DMA experiments a static stress of 1.50 MPa was applied over a dynamic stress of 1.00 MPa of amplitude that allowed maintaining the sample tough. TMA was conducted on a TA Instruments TMA Q400 apparatus. In the TMA experiments a small force of 10 mN was applied to the rectangular samples, also 4 mm width and 25 mm distance between clamps, in order to keep them vertical during heating from 20 to 120 °C at a rate of 2 °C min^{-1}.

Results and discussion

Thermogravimetric analysis

TG is a common method to investigate the thermal decomposition and stability of polymeric systems. Figure 1 shows the TG data for the studied P(VDF–CTFE–TrFE) terpolymer films. For all the samples, only single decomposition stage was observed. No mass loss was found around 100 and 150 °C, indicating the absence of water and DMF in the samples after drying. The major mass loss process occurred in the region between 400 and 550 °C.
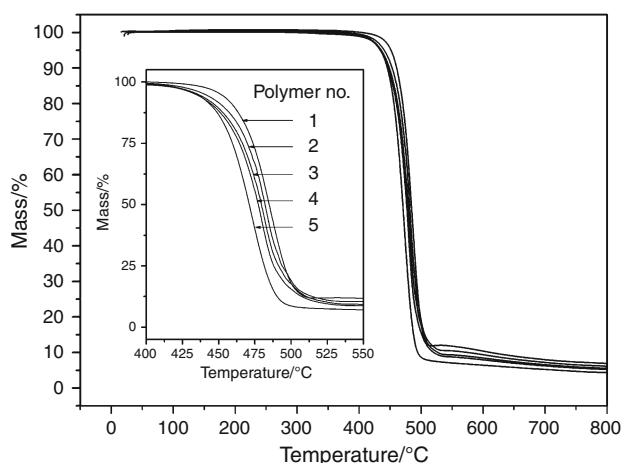

Fig. 1 TG curves of the P(VDF–CTFE–TrFE) films, obtained at 10 °C min^{-1}, The inset plot is an amplified image of the TG curves

After the primary degradation mechanism, less than 12% of residual mass remained. In general, the process of thermal decomposition can be characterized by a number of experimental indicators. From the TG profile, at least three characteristic temperatures can be obtained [34]: (I) the initial temperature, $T_{initial}$, which is defined as the temperature at which the experimental curve diverges from the tangent line that the mass evolution follows before degradation, (II) the onset temperature, T_{onset}, that is calculated by extending the pre-degradation portion of the curve to the point of interception with a line drawn as a tangent to the steepest portion of the mass curve occurring during degradation, and (III) the temperature of half decomposition, T_{half}, the temperature at which the loss of mass during pyrolysis reaches 50% of its final value (in this study, we regard the amount of char residue at 800 °C as the final value). In addition, the differential degradation curve (the first-order derivative of TG curve) can give us further information about the rate of decomposition. Figure 2 shows the DTG data for the samples, the peak temperature in DTG curve, T_{max}, corresponds to the temperature of maximum mass loss rate.

Table 2 summarized the data of degradation processes of the polymers. A trend can be easily found that all the characteristic temperatures and residual mass (at the same temperature) increased gradually with the order from polymer 1 to 5. That means the thermal stability of the terpolymer enhanced slightly with a decrease in CTFE or chlorine content. In fact, the chlorine content usually plays an important role on dropping the thermal stability of polymer systems. For example, among polyethylene (PE), chlorinated polyethylene (CPE) and poly(vinyl chloride) (PVC), the CPE generally decomposes at a lower temperature than PE during heating; however, the PVC is often more easily to thermally decompose than CPE [35]. This is because the C–Cl bonds are usually the weak points of the polymer chains, during heating, they favor to hemolytic break and often initiate the chain reactions to decompose the polymers [36].

TG is an excellent tool for studying the thermal degradation kinetics. It is widely used because of its experimental simplicity and the wealth of information obtained from a simple thermogram. From Fig. 1, the information about the kinetics of the loss process can be investigated. The expression for the thermal decomposition of a homogeneous system has the following general form:

$$\frac{d\alpha}{dt} = k(T)f[a(t)]$$

where α represents the reaction extent of the component of the sample under degradation, t is the time, the rate constant $k(T)$ changes with absolute temperature T according to the Arrhenius equation. $f(\alpha)$ represents the
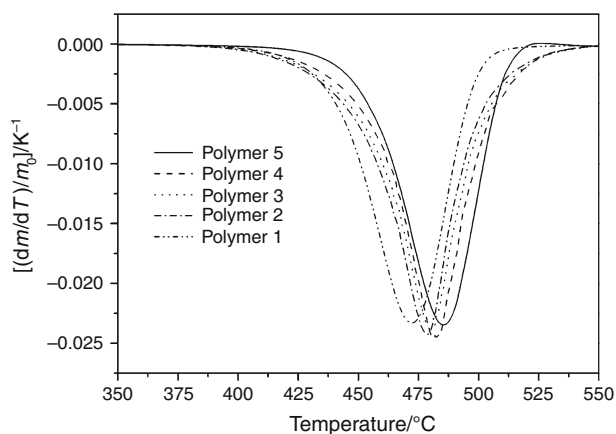
Fig. 2 The DTG curves of the P(VDF–CTFE–TrFE) films, obtained at 10 °C min^{-1}

Fig. 3 Representation of the data of Fig. 1 in order to use the Broido method. The points are experimental results and the solid lines are the linear fitting of the process

net results of elementary steps, as the polymer degradations are often chain reactions. For solid state reactions $f(\alpha) = (1-\alpha)^n$, where n is the order of reaction, assumed to remain constant during the degradation process. Under the assumption of $n = 1$ and applying the Broido method, the expression for the thermal decomposition of the polymer system can be written as follow [34]:

$$\text{In}[-\text{In}(1 - \alpha)] = -\frac{E_a}{RT} + const$$

where E_a is the activation energy of the degradation process, R is the gas constant (8.314 J mol^{-1} K^{-1}). In this method a straight line should be observed in the plot of ln[−ln(1−α)] versus T^{-1} with a slope of $-E_a R^{-1}$. Figure 1 was used to calculate α(T) and Fig. 3 shows the ln[−ln(1−α)] versus $10^3 T^{-1}$ plot for the studied terpolymers. The data, ranging from 450 to 490 °C with step of 5 °C, were linearly fitted with $R > 0.99$. From the slope of the fitting lines the activation energy of the terpolymers was obtained and listed in Table 2. It is observed that, except for polymer 1 and 2, the value of E_a computed using this method exhibits similar trend of that the characteristic temperatures of the terpolymers drops with the increasing CTFE content. However, for polymer 1, its E_a value is even larger than that of polymer 4. As for this we should recognize that the thermal degradation is quite complicated,
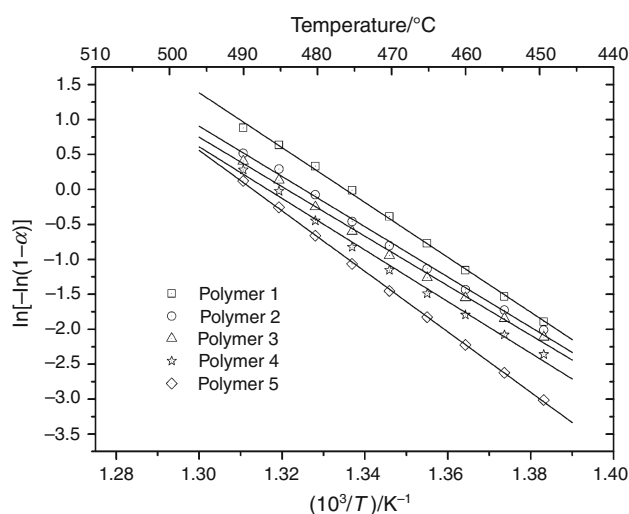
besides the CTFE content, some other factors may have affected the processes.

Differential scanning calorimetry

The DSC measurement was used to characterize the phase transitions and crystalline structures of the terpolymers. Figure. 4 records the DSC traces of the samples at the first heating run. For all the curves, only one endothermic peak is apparent, which results from the melting process. A weak F–P transition is found in polymers 4 and 5, indicating the existence of a small amount of β-phase in them. Table 3 summarizes the phase transition data, where, T_m and ΔH_m are the peak temperature and enthalpy associated with the melting behavior, respectively; and T_c and ΔH_c are the peak temperature and enthalpy corresponding to the F–P transition, respectively.

It shows clearly that as the polymer with higher concentration of CTFE, both the melting temperature and enthalpy of the terpolymer decrease continuously. This agrees with the previous studies [29–31], suggesting the CTFE units, serve as defects; destroy the crystalline

Table 2 Data summary of degradation processes of the terpolymer films

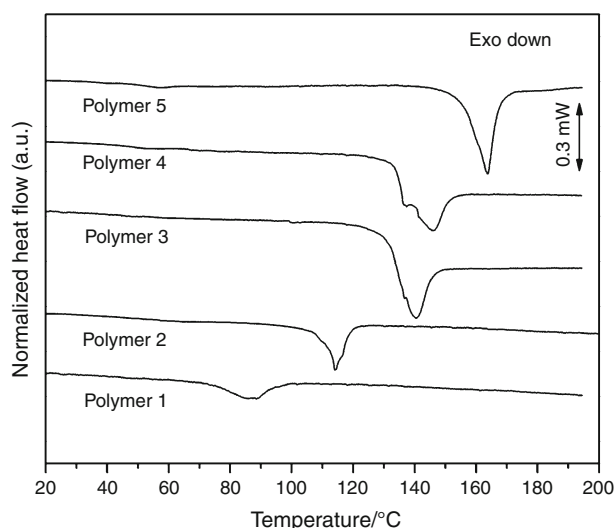| Polymer no.	$T_{initial}$/°C	T_{onset}/°C	T_{half}/°C	T_{max}/°C	E_a /kJ mol^{-1}	Weight remaining/% (±0.1)					
						400 °C	450 °C	475 °C	500 °C	550 °C	800 °C
1	381.1	446.8	470.2	471.9	4.72	98.9	86.6	39.9	8.7	7.1	4.2
2	383.4	450.9	476.3	478.4	4.30	99.1	88.1	55.5	15.6	8.8	5.1
3	384.8	453.7	478.4	479.7	4.28	99.2	89.2	60.0	17.6	9.3	5.4
4	389.7	457.5	480.9	481.5	4.44	99.5	91.5	66.6	19.1	10.5	6.0
5	405.6	465.2	483.6	485.3	5.20	100.0	95.5	72.8	18.0	11.9	6.8

Fig. 4 The DSC traces of the P(VDF–CTFE–TrFE) terpolymers at the first heating run

Table 3 Data summary of the first heating DSC curves for the terpolymer films

Polymer no.	$T_m/°C$	$\Delta H_m/J\ g^{-1}$	$T_c/°C$	$\Delta H_c/J\ g^{-1}$
1	87.3	−4.39	N.A.	N.A.
2	114.3	−5.70	N.A.	N.A.
3	140.5	−13.88	N.A.	N.A.
4	146.2	−14.79	52.7	−0.17
5	163.4	−17.71	57.8	−0.56

structures of the terpolymers. On the other hand, the curie transition was very weak in polymer 5 and 4, and even disappeared in polymer 3, 2, and 1, indicating that only a small amount of CTFE units can eliminate the polar phase remarkably. This is different from the P(VDF–CTFE–TrFE) terpolymers prepared from direct-polymerization process [19, 22, 24], in which the CTFE units show a lower efficiency to eliminate the F–P transition. It is mainly because the indirect-polymerization process in this study may have brought more region-defects to the polymers [30, 31].

The degree of crystallinity (X_c) can be calculated by the following formula:

$$X_c = \Delta H_m / \Delta H_{m(100\%)}$$

In this study, however, the value of $\Delta H_{m\ (100\%)}$ (the melting enthalpy of 100% crystalline of the polymer) is unknown. Yet it is reasonable to believe that the values of $\Delta H_{m\ (100\%)}$ for the terpolymers are almost the same. Under this assumption, the crystallinity of the terpolymer decreases with an increasing content of CTFE. In fact, this has been demonstrated by WXRD in previous study [29, 30].

Probably because the solution-cast terpolymer films did not follow an annealing process, morphologically, the shape of their melting peaks (especially the melting peaks of polymer 4, 3 and 2) is complex; this reflects the presence of complicated crystalline organizations in the polymers, which may include the co-existence of the crystalline structures with varied size or in different phases or both the former cases. In general, what structures the polymers possess are strongly affected by the processing conditions which they undergo. The relatively complicated and broad melting peaks also suggest the imperfect crystals in the solution-cast films.

Dynamic mechanical analysis

DMA is employed to investigate the molecular motions and the related macroscopic viscoelastic behavior of the polymers. In a DMA test, the sample is subjected to repeated small-amplitude strains in a cyclic manner. The storage modulus (E'), the loss modulus (E'') and the loss factor ($\tan\delta = E''/E'$) are measured. E' is a measure of the energy stored elastically whereas E'' is a measure of the energy lost as heat. $\tan\delta$ is also called the damping and it indicates how efficiently the material loses energy to molecular rearrangement and the internal friction. The $\tan\delta$ curve reveals various types of mechanical relaxations associated with the molecular motions. Figure 5 displays the temperature dependence of the storage modulus and the loss factor at a fixed frequency of $f = 1$ Hz.

As can be seen, the storage modulus for all samples decreases with temperature as the samples pass from the glassy to the rubbery state. In the same temperature, the polymer includes higher CTFE content will have a lower storage modulus. The stiffness of polymer 1 is so low that it was breakdown when heated to only around 50 °C whereas polymer 5 still has a value of E' over 200 MPa in this
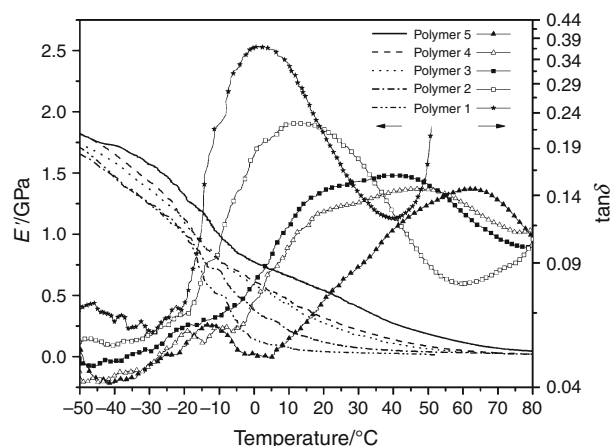

Fig. 5 DMA spectra (storage modulus and loss factor) of the P(VDF–CTFE–TrFE) terpolymers measured at 1 Hz

temperature. One can easily correlate this behavior with the crystallinity of the samples, because the polymer with a lower CTFE content has a higher degree of crystallinity which is beneficial to enhance stiffness of the materials. However, this seems not to be so apparent when at low temperature due to the molecular chains are frozen both in amorphous and crystalline fraction before the glass transition occurring.

The mechanical loss spectra of the samples are more complicated to analysis. In general, the loss peaks can be divided into two groups according to the located temperature. In the high temperature region, a broad and pronounced relaxation peak was found. This process, labeled α or α_c, is mainly associated with the molecular motions, involving rotational and translation mobility of the chain stems [37], within the crystalline fraction. However, due to their semi-crystalline nature of the terpolymers, the cooperative mobility of molecular chains in the amorphous region as well as the crystal-amorphous interface should accompany this process. Moreover, the F–P phase transition should also make contributions to α_c process in the case of polymer 5 and 4 due to their T_c just locate at this process. The α_c relaxation peak reduces its intensity and shifts to a higher temperature as polymer with less CTFE content, because the enhanced crystallinity prefers to restrict the movement of molecular chains. In the low temperature region, polymer 5 exhibits an obvious relaxation peak located at about -13 °C, this process, assigned to the dynamic glass transition of segments in the amorphous phase, is less prominent than the α_c relaxation and usually labeled β or α_a. The α_a process is significantly weakened in polymer 4 and 3 and disappeared in polymer 2 and 1. It is conceivable that, as the fraction of amorphous phase increases greatly with high concentrations of CTFE in the polymer, the crystalline phase has been destroyed to a more imperfect and diffuse state, which makes the α_a and α_c relaxations in the polymers of high CTFE content merging into a new broad relaxation peak with the contributions from glass transition of amorphous phase, the segmental motion in the crystalline phase and the cooperative mobility of the interface.

Thermal mechanical analysis

From a practical point of view, the TMA give information about the dimensional stability of the terpolymer films along the temperature axis that may be useful for certain applications.

Figure 6 shows the TMA results of the samples. The relative change in sample length, $\Delta l = (l-l_0)/l_0$, was measured during continuous heating at 2 °C min^{-1} and normalized to the initial sample length l_0 at 20 °C. As can be observed, the sample length shows more than one regime of
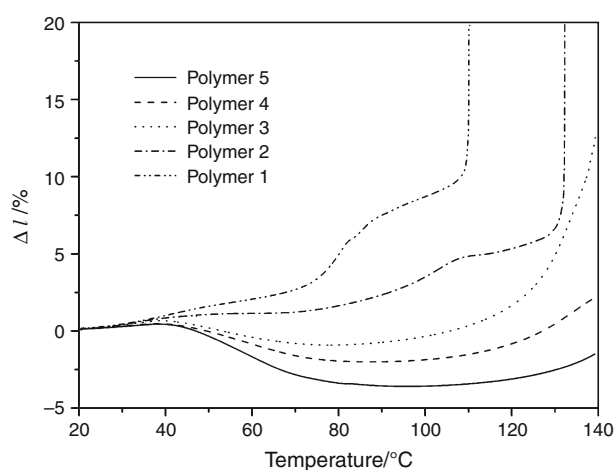

Fig. 6 TMA traces, showing the variation in the distance between clamps (Δl) with temperature, relatively to the initial length, in samples subjected to a small load (10 mN). Temperature rate: 2 °C min^{-1}

variation for all the polymers. From 20 to 40 °C the sample length slightly increases due to the thermal expansion. Close examination reveals that Δl is linearly dependent on temperature and the slope decreases gradually from polymer 1–5 because of the enhancement of stiffness. When heated to above 40 °C, surprisingly, all the samples undergo a process of contraction in length to varying extent: the shrinkage is weak in polymer 1 and 2 but significant in polymer 3, 4 and 5, a lower CTFE content of sample has a higher degree of contraction in length. After contraction, the samples followed by a non-linear regime of pronounced thermal expansion due to soften at high temperature. It is clear that the polymer with a higher CTFE content softened at a lower temperature because of its lower melting point.

In general, the behavior of contraction upon heating is very common in retractable films used in packaging [38], usually produced in polyethylene, due to the release of the orientation induced by the stretching of the films during their formation processes. However, in this study only a simple solution-cast method without any other processing was used to prepare the samples. Therefore, the reasons for this shrinkage behavior should be related to the process of casting. Indeed, solution-cast thermoplastic thin films inherently generate internal stress in the plane of them [39–42]. Polymeric coatings usually shrink during and after solidification due to solvent evaporation, coating adhesion, however, prevents shrinkage from occurring freely; this frustration of in-plane shrinkage leads to a tensile stress in the plane of the coating. Croll [41, 42] proposed that the internal strain induced by the constrained shrinkage depends on the solvent loss after the solidification point; he referred to this point at which the polymer molecules can no longer f1ow to fill the gaps left by the lost solvent molecules. In this study, the solution-cast terpolymer films

crystallized to varying degrees depending on the CTFE content. It is believe that the strain tends to be greater for polymer film with higher degree of crystallinity, because the crystallization should give rise to a higher viscosity of the polymer/solvent system, resulting in an earlier solidification point and the larger volume of solvent lost after it. Alternatively, the formation of crystallites should give closer packing of the polymer chains, leading to greater volume of shrinkage. Therefore, a lower CTFE content of polymer film should generate a greater tensile strain/stress during drying. From a thermodynamic point of view, these solution-cast polymer films are metastable for their molecule chains are frozen in a tensile state at room temperature. To lower free energy, the polymer system has to overcome an energy barrier to initiate the loosing of the tension in molecule chains. When heated to a certain temperature, the system can overcome this barrier and then releases tensile stress to an equilibrium state. Thus, it is not difficult to understand that the polymer films experienced a contraction process after a slight of thermal expansion upon heating, and that for the greater release of tensile stress the lower CTFE content of film shrank to a larger extent.

Few studies have discussed the molecular origin of the geometrical recovery in solution-cast films of semicrystalline polymers during heating. In this study, the α_a and α_c relaxation gradually merge together as CTFE content increasing, so the CTFE content or the crystallinity of the polymer should play a significant role here. It is suggested that the origin of the contraction of polymer films with low CTFE content (Polymer 5, 4 and 3) is more likely to be related with the occurrence of the α_c relaxation, which accompanies cooperative diffusion processes in the amorphous phase and the interface, resulting in the loosing of the tension in molecule chains to lower free energy of the polymer system. As for the polymer with high CTFE content (Polymer 1 and 2), the α_a relaxation should make more contribution to initiate the shrinkage process due to their greater amorphous fraction.

Conclusions

Thermal behavior of the solution-cast P(VDF–CTFE–TrFE) terpolymer films with different CTFE content have been characterized in an integrated way by a series of thermal analysis techniques. The results suggest that the CTFE content affect thermal properties of the terpolymers:

(a) The terpolymers exhibited a relatively stable behavior with a single degradation process at temperature above 400 °C. A lower CTFE content gives the polymer slightly higher thermal stability probably due to the instability of C–Cl bond during heating.

(b) The introduction of CTFE units decreases the melting temperatures, fusion enthalpy and crystallinity of the terpolymers. On the other hand, due to the indirect-polymerization process brings the high percentage of regiodefects to the polymer, CTFE units show a high efficiency to eliminate the F–P transition.

(c) Dynamic mechanical analysis detected a relatively weak α_a relaxation (attributed to the dynamic glass transition, located at the low temperature) and a broad α_c relaxation (mainly assigned to the molecular motions within the crystalline structure, located at the high temperature) in the samples of low CTFE content. These two relaxation processes completely mixed together in the samples of high CTFE content, revealing the crystalline structures in the polymer become a more imperfect and diffuse state as CTFE units increasing. The semi-crystalline nature of the terpolymers suggests the molecular mobility in the crystalline fraction should accompany the cooperative processes in the amorphous region and the interface. The higher degree of crystallinity of the polymer with less CTFE units account for its enhanced stiffness.

(d) The solution-cast terpolymer films experienced a contraction process after a slight amount of thermal expansion upon heating in order to release the internal tensile strain/stress generated during solidification process. The higher crystallinity of the polymer film generated the greater strain/stress, leading to the larger degree of shrinkage. Also, the higher melting point of the polymer with less CTFE units allows it soften at a higher temperature. Depending on the crystallinity, the molecule origin of shrinkage process should be mainly related with the α_c relaxation in the case of polymer with low CTFE units; however, the α_a relaxation should make more contribution in the case of polymer with high CTFE units.

References

1. Herbert JM, Glass AM, Wang TT. The application of ferroelectric polymers. New York: Chapman & Hall; 1988.
2. Naber RCG, Tanase C, Blom PWM, Gelinck GH, Marsman AW, Touwslager FJ, et al. High-performance solution-processed polymer ferroelectric field-effect transistors. Nat Mater. 2005;4(3):243–8.
3. Stadlober B, Zirkl M, Beutl M, Leising G, Bauer-Gogonea S, Bauer S. High-mobility pentacene organic field-effect transistors with a high-dielectric-constant fluorinated polymer film gate dielectric. Appl Phys Lett. 2005;86(24):242902. doi:10.1063/1.1946190.

4. Müller K, Paloumpa I, Henkel K, Schmeisser D. A polymer high-k dielectric insulator for organic field-effect transistors. J Appl Phys. 2005;98(5):056104. doi:10.1063/1.2032611.

5. Chu B, Zhou X, Ren K, Neese B, Lin M, Wang Q, et al. A dielectric polymer with high electric energy density and fast discharge speed. Science. 2006;313(5785):334–6. doi:10.1126/science.1127798.

6. Lovinger AJ. Ferroelectric polymers. Science. 1983;220(4602):1115–21. doi:10.1126/science.220.4602.1115.

7. Kawai H. The piezoelectricity of poly(vinylidene fluoride). Jpn J Appl Phys. 1969;8(7):975–6.

8. Bergman JG, McFee JH, Crane GR. Pyroelectricity and optical second harmonic generation in poly(vinylidene fluoride) films. Appl Phys Lett. 1971;18(5):203–5.

9. Tamura M, Ogasawara K, Ono N, Hagiwara S. Piezoelectricity in uniaxially stretched poly (vinylidene fluoride). J Appl Phys. 1974;45(9):3768–71.

10. Yagi T, Tatemoto M, Sako J-i. Transition behavior and dielectric properties in trifluoroethylene and vinylidene fluoride copolymers. Polym J. 1980;12(4):209–23.

11. Bune AV, Fridkin VM, Ducharme S, Blinov LM, Palto SP, Sorokin AV, et al. Two-dimensional ferroelectric films. Nature. 1998;391(6670):874.

12. Zhang QM, Bharti V, Zhao X. Giant electrostriction and relaxor ferroelectric behavior in electron-irradiated poly(vinylidene fluoride-trifluoroethylene) copolymer. Science. 1998;280(5372):2101.

13. Tashiro K, Tadokoro H, Kobayashi M. Structure and piezoelectricity of poly(vinylidene fluoride). Ferroelectrics. 1981;32(1):167–75.

14. Nalwa HS. Recent developments in ferroelectric polymers. J Macromol Sci Poly Rev. 1991;C31(4):341–432.

15. Furukawa T. Structure and functional properties of ferroelectric polymers. Adv Colloid Interface. 1997;71–72:183–208. doi:10.1016/s0001-8686(97)90017-8.

16. Higashihata Y, Sako J, Yagi T. Piezoelectricity of vinylidene fluoride–trifluoroethylene copolymers. Ferroelectrics. 1981;32(1):85–92.

17. Furukawa T. Ferroelectric behavior in the copolymer of vinylidenefluoride and trifluoroethylene. Jpn J Appl Phys. 1980;19(2):109–12.

18. Yamada T, Ueda T, Kitayama T. Ferroelectric-to-paraelectric phase transition of vinylidene fluoride-trifluoroethylene copolymer. J Appl Phys. 1981;52(2):948–52.

19. Chung TC, Petchsuk A. Ferroelectric VDF/TrFE/CTFE terpolymers: synthesis and electric properties. In: Bar-Cohen Y, editor. Smart structures and materials 2001: electroactive polymer actuators and devices: The International Society for Optical Engineering; 2001. p. 117–24.

20. Xu H, Cheng ZY, Olson D, Mai T, Zhang QM, Kavarnos G. Ferroelectric and electromechanical properties of poly(vinylidene–fluoride–trifluoroethylene–chlorotrifluoroethylene) terpolymer. Appl Phys Lett. 2001;78(16):2360.

21. Chung TC, Petchsuk A, Taylor GW. Ferroelectric polymers with large electrostriction; based on semicrystalline VDF/TrFE/CTFE terpolymers. Ferroelectrics Lett. 2001;28(5):135–43.

22. Chung TC, Petchsuk A. Synthesis and properties of ferroelectric fluoroterpolymers with Curie transition at ambient temperature. Macromolecules. 2002;35(20):7678–84. doi:10.1021/ma020504c.

23. Xia F, Cheng Z, Xu H, Li H, Zhang Q, Kavarnos GJ, et al. High electromechanical responses in a poly(vinylidene fluoride-trifluoroethylene-chlorofluoroethylene) terpolymer. Adv Mater. 2002;14(21):1574–7.

24. Buckley GS, Roland CM, Casalini R, Petchsuk A, Chung TC. Electrostrictive properties of poly(vinylidenefluoride–trifluoroethylene–chlorotrifluoroethylene). Chem Mater. 2002;14(6):2590–3. doi:10.1021/cm0116471.

25. Klein RJ, Runt J, Zhang QM. Influence of crystallization conditions on the microstructure and electromechanical properties of poly(vinylidene fluoride–trifluoroethylene–chlorofluoroethylene) terpolymers. Macromolecules. 2003;36(19):7220–6. doi:10.1021/ma034745b.

26. Bauer F, Fousson E, Zhang QM, Lee LM. Ferroelectric copolymers and terpolymers for electrostrictors: synthesis and properties. IEEE Trans Diel Elec Insu. 2004;11(2):293–8.

27. Xu H, Shen D, Zhang Q. Structural and ferroelectric response in vinylidene fluoride/trifluoroethylene/hexafluoropropylene terpolymers. Polymer. 2007;48(7):2124–9. doi:10.1016/j.polymer.2007.02.035.

28. Hulburt JD, Feiring AE. Trifluoroethylene deflagration. Chem Eng News. 1997;75(51):6.

29. Lu Y, Claude J, Neese B, Zhang Q, Wang Q. A modular approach to ferroelectric polymers with chemically tunable curie temperatures and dielectric constants. J Am Chem Soc. 2006;128(25):8120–1. doi:10.1021/ja062306x.

30. Lu Y, Claude J, Zhang Q, Wang Q. Microstructures and dielectric properties of the ferroelectric Fluoropolymers synthesized via reductive dechlorination of poly(vinylidene fluoride-co-chlorotrifluoroethylene)s. Macromolecules. 2006;39(20):6962–8. doi:10.1021/ma061311i.

31. Wang Z, Zhang Z, Chung TCM. High dielectric VDF/TrFE/CTFE terpolymers prepared by hydrogenation of VDF/CTFE copolymers:synthesis and characterization. Macromolecules. 2006;39(13):4268–71. doi:10.1021/ma060738m.

32. Lu Y, Claude J, Norena-Franco LE, Wang Q. Structural dependence of phase transition and dielectric relaxation in ferroelectric poly-(vinylidene fluoride–chlorotrifluoroethylene–trifluoroethylene)s. J Phys Chem B. 2008;112(34):10411–6. doi:10.1021/jp802413g.

33. Li H, Tan K, Hao Z, He G. Preparation and crystallization behavior of poly(vinylidene fluoride-ter-chlorotrifluoroethylene-ter-trifluoroethylene). J Appl Polym Sci (Accepted).

34. Sencadas V, Lanceros-Me'ndez S, Mano JF. Thermal characterization of a vinylidene fluoride-trifluoroethylene (75–25) (%mol) copolymer film. J Non-Cryst Solids. 2006;352(50–51):5376–81.

35. Varma AJ, Deshpande SV, Kondapalli P. A comparative study of the thermal behavior of PVC, a series of synthesized chlorinated polyethylenes and HDPE. Polym Degrad Stabil. 1999;63(1):1–3. doi:10.1016/s0141-3910(98)00051-2.

36. Zulfiqar S, Zulfiqar M, Rizvi M, Munir A, McNeill IC. Study of the thermal degradation of polychlorotrifluoroethylene, poly(vinylidene fluoride) and copolymers of chlorotrifluoroethylene and vinylidene fluoride. Polym Degrad Stabil. 1994;43(3):423–30. doi:10.1016/0141-3910(94)90015-9.

37. Mano JF, Sencadas V, Costa AM, Lanceros-Méndez S. Dynamic mechanical analysis and creep behaviour of β-PVDF films. Mater Sci Eng A 2004;370(1–2):336–40. doi:10.1016/j.msea.2002.12.002.

38. Sencadas V, Lanceros-Méndez S, Mano JF. Characterization of poled and non-poled β-PVDF films using thermal analysis techniques. Thermochim Acta. 2004;424(1–2):201–7.

39. Francis LF, McCormick AV, Vaessen DM, Payne JA. Development and measurement of stress in polymer coatings. J Mater Sci. 2002;37(22):4717–31. doi:10.1023/a:1020886802632.

40. Diane M, Whitmore PM, editors. The development of internal stress in films of thermoplastic polymers cast from solution. Materials Research Society Symposium Proceedings; 1995.

41. Croll SG. Internal stress in a solvent-cast thermoplastic coating. J Coat Technol. 1978;50(638):33–8.

42. Croll SG. The origin of residual internal stress in solvent-cast thermoplastic coatings. J Appl Polym Sci. 1979;23(3):847–58. doi:10.1002/app.1979.070230319.